LOW-LOSS ANALOG FIBER-OPTIC LINKS

C. H. Cox III, D. Z. Tsang, L. M. Johnson and G. E. Betts

Lincoln Laboratory, Massachusetts Institute of Technology
Lexington, Massachusetts 02173-9108

ABSTRACT

Experimental and theoretical studies of high-performance fiber-optic links are reported. For the experimental directly modulated link, the measured electrical insertion gain was -4.9 dB at a bandwidth of 1500 MHz, and 0.3 dB at a bandwidth of 200 MHz. For the experimental externally modulated link operating at a bandwidth of 800 MHz, the calculated electrical insertion gain based on actual device parameters is -1.0 dB, while at 150 MHz a gain of 6.0 dB is expected. Both links have no active amplification. The directly modulated links have higher noise figures because of the high relative intensity noise of the diode laser.

I. INTRODUCTION

The two most common modulation methods presently used in analog fiber-optic links are direct modulation of a diode laser and external modulation of a cw laser. Comparison of the fundamental limits of these two methods is facilitated by measurement of incremental modulation efficiency [1]:

$$\mathrm{IME} \triangleq \frac{p_o^2}{p_{in,a}}, \tag{1}$$

where p_o is the fiber-coupled modulated optical power from the modulating device and $p_{in,a}$ is the available RF power from the modulation source. The IME provides a measure of modulated optical power output in relation to input power available. For both modulation methods, the modulated optical power is proportional to either the current or voltage of the RF source. Since we wish to express the IME in terms of available RF power, the square of modulated optical power appears in the expression for IME. Although direct and external modulation methods can achieve similar results, we have reported significant differences in their functional dependence on device parameters. In particular, the IME for external modulation is proportional to the square of the optical bias power, whereas the IME for direct modulation is, at best, independent of optical bias power.

We have reported [1] that IME for direct and external modulation can be expressed as the product of a factor that includes various device parameters and a factor that includes the device resistance. In this paper, the resistance of the modulating device is assumed to be matched to the source impedance, R_{in}. Consequently, it is useful to express IME from Eq. (1) as

$$\mathrm{IME} \triangleq \frac{p_o^2}{p_{in,a}} \triangleq \frac{H^2}{R}, \tag{2}$$

where H is the product of the electrooptic conversion efficiency (in W/A) and R is the effective input resistance of the laser or modulator (in Ω).

II. INCREMENTAL MODULATION EFFICIENCY

Previously derived expressions for IME with direct and external modulation will be expressed in terms of H and R. For simplicity, the frequency dependence of the IME will be neglected to the extent possible, and discussion will apply to the midband value.

For direct modulation, it was shown [1] that

$$\frac{p_o^2}{p_{in,a}} = \eta_{LB}^2 \frac{1}{R_L}, \tag{3}$$

where η_{LB} is the fiber-coupled diode laser incremental slope efficiency and R_L is the laser series resistance. Thus, we immediately obtain $H = \eta_{LB}$ and $R = R_L$. Typically, the laser series resistance is much smaller than the source impedance. To achieve the potential improvement in IME offered by a low value of R_L and simultaneously achieve a low return loss, some form of lossless impedance matching is required. A straightforward implementation is a step-down transformer whose turns ratio N_L is chosen such that $N_L^2 R_L = R_{in}$.

Equation (3) can be used to plot contours of constant IME in the H-R plane, as shown in Fig. 1. In general, the higher the IME, the higher the link gain, or the lower the link loss. Since there is little if any practical advantage to operating a directly modulated diode laser with $R_L > R_{in}$ (assuming $R_{in} = 50\ \Omega$), we do not plot the contours in this range. The limit on η_{LB} (η'_{LB-max} shown in Fig. 1) can be derived by expressing η_{LB} as the product of the diode laser incremental slope efficiency η'_{LB} and the laser-to-fiber optical coupling efficiency t_{lf}. Clearly, the maximum value of t_{lf} is 1. If all electrons in a uniformly pumped diode laser are converted to photons, η'_{LB} can be shown [2] to be equal to $hc/q\lambda$, where q is the electron charge, λ is the lasing wavelength, h is Planck's constant, and c is the speed of light. For $\lambda = 1.3\ \mu m$, $\eta'_{LB-max} \cong 0.95$ W/A. Thus, $\eta_{LB\text{-}max}$ is limited by

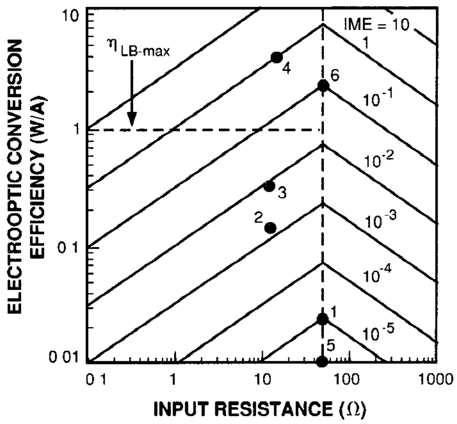

Fig. 1. Plots of constant IME vs electrooptic conversion efficiency H and input resistance R of the modulating device. For $R \neq R_{in}$, lossless matching to R_{in} is assumed. For $R = R_{in}$, a resistor is used to make the effective resistance of the resistor/device combination equal to R_{in}. The horizontal dashed line indicates the maximum H for a directly modulated laser operating at $\lambda = 1.3$ µm. The vertical dashed line indicates the characteristic resistance of the RF source. For $R < R_{in}$, the only contours plotted are for direct modulation and series-matched external modulation. For $R > R_{in}$ the only contours plotted are for parallel-matched external modulation. Numbered points represent experimental results, discussed in the text.

fundamental constraints. On the other hand, the value of R_L is practically but not fundamentally limited.

Commercially available fiber-coupled lasers typically have $\eta'_{LB} = 0.25$ W/A, $t_{lf} = 0.1$, and $R_L = 10\ \Omega$. However, these devices have no internal lossless RF matching, and their packaging precludes effective external lossless matching. Therefore, the only practical match to these devices is via a series resistor R'_L, such that $R_L + R'_L = R_{in}$. The point corresponding to these conditions with $R_{in} = 50$ is indicated by data point 1 in Fig. 1.

Recently, we have achieved a t_{lf} of 0.7 for a 50/125-µm multimode fiber by forming an integral, lenslike end on the optical fiber. This experiment also used a step-down transformer with $N_L = 2$ to implement a low-loss impedance match to the laser. The η_{LB} was 0.20 W/A, and R_L was ~10 Ω. Point 2 in Fig. 1 corresponds to these conditions.

Tsang has developed a laser with a high slope efficiency (0.55 W/A) and a low threshold at a wavelength of 1.3 µm [3]. If this laser is operated with high-efficiency fiber coupling and a low-loss impedance match, then the IME indicated by point 3 in Fig. 1 should be achievable. The directly modulated link described in Section III is an experimental confirmation of this case.

The IME for a lumped-element impedance-matched Mach-Zehnder (MZ) interferometric external modulator was also reported [1]. Traveling wave modulators were not considered. For the lumped-element device, we looked at both series and parallel matches. In the series match case, R_m is the effective series resistance of the modulator, including both the intrinsic modulator resistance and any series resistance added to improve the match. For this case, the IME was expressed as

$$\frac{p_o^2}{p_{in,a}} = \left(\frac{t_{ff} P_I \pi}{2V_\pi}\right)^2 \frac{1}{s^2 C_m^2 R_m} \,, \tag{4}$$

where t_{ff} is the excess optical insertion loss of the modulator, P_I is the input optical power, V_π is the modulator switching

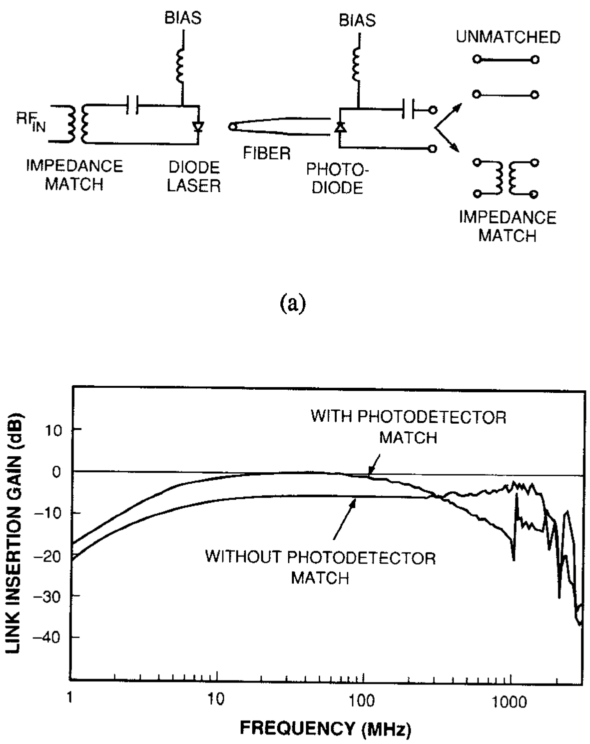

Fig. 2. (a) Schematic diagram of the directly modulated link used in experiments. Measurements were made with and without impedance matching. (b) Link insertion gain vs frequency for the directly modulated link.

voltage, s is the complex frequency, and C_m is the modulator capacitance. Rearranging the terms of Eq. (4) using the variables in Eq. (2), we obtain

$$H = \frac{t_{ff} P_I \pi}{2V_\pi s C_m} \tag{5}$$

and

$$R = \frac{R_{in}}{N_m^2} = R_m \,, \tag{6}$$

where N_m is the turns ratio of the matching transformer. The expression of H in Eq. (5) differs from H for the directly modulated links because of its intrinsic frequency dependence and its optical bias power dependence. However, the expression of R in Eq. (6) has the same functional form as for the directly modulated links. Note that the optical wavelength dependence is included in V_π.

The contours of constant IME for the series match case are the same as those for the directly modulated diode laser case, except for the limit on H. The series match case has not been explored extensively. We have reported one implementation [4], in which $P_I = 55$ mW, $V_\pi = 0.7$ V, $t_{ff} = 0.35$, $C_m = 45$ pF, $R_m = 16\ \Omega$, $N_m \cong 2$, and the operating

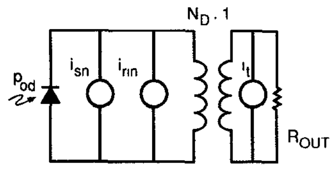

(a)

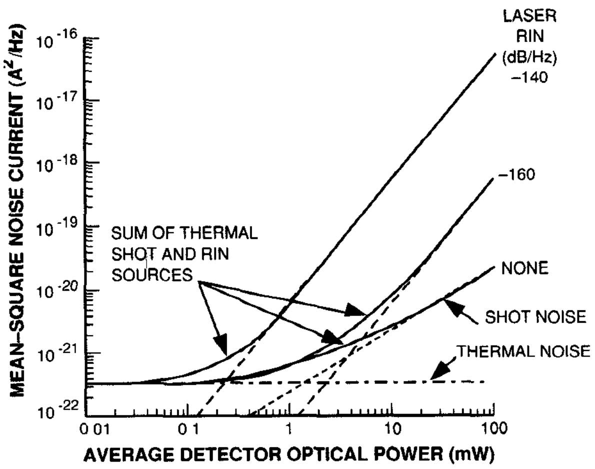

(b)

Fig. 3. (a) Small-signal noise model with major noise sources, which are shot noise, laser RIN, and thermal noise, referred to the detector end of the link. (b) Plots of mean-square noise current vs average optical power at the photodiode.

frequency is 60 MHz. The IME corresponding to these conditions is represented by point 4 in Fig. 1.

For the parallel match case, the IME has been expressed as

$$\frac{p_o^2}{p_{in,a}} = \left(\frac{t_{ff} P_I \pi}{2V_\pi}\right)^2 R_p \,, \tag{7}$$

where R_p is a matching resistor in parallel with the modulator. A parallel match requires $N_m^2 R_p = R_{in}$, so Eq. (7) can be expressed as follows using the variables of Eq. (2):

$$H = \frac{t_{ff} P_I \pi R_{in}}{2V_\pi} \tag{8}$$

and

$$R = R_{in} N_m^2 = \frac{R_{in}^2}{R_p} \,. \tag{9}$$

TABLE 1

Performance	Modulation			
	Direct	External	Direct	External
Bandwidth (MHz)	200	150	1500	800
RF Insertion Gain (dB)	0.3	6.0*	-4.9	-1.0†
Noise Figure (dB)	30.1	15.1*	35.1	19†

*Estimated
†Experiment in progress

The conversion efficiency of the parallel-matched modulator, like the series-matched modulator, depends on the optical bias power. Unlike the series match case, the parallel match case has no explicit frequency dependence, but it does depend on frequency through the modulator design, since V_π is proportional to bandwidth. The parallel match case differs from both the series match and direct modulation cases by requiring a step-up transformer to maximize IME.

Contours of constant IME for the parallel match case are shown in Fig. 1. Since there is little if any practical advantage to operating the parallel matched modulator with $R_p < R_{in}$ (assuming $R_{in} = 50\ \Omega$), we do not plot the contours in this range. Common practice has been to use external modulators with $V_\pi \cong 5$ V operated with $P_I = 1$ mW and $N_m = 1$, i.e., $R_p = 50\ \Omega$. If we continue to assume that $t_{ff} = 0.35$, then the IME for these conditions can be plotted as point 5 in Fig. 1.

The modulator referred to above in the discussion of the series match case has also been operated with a parallel match, with $N_m = 1$ and $R_p = R_{in} = 50\ \Omega$. The IME corresponding to these conditions is shown by point 6 in Fig. 1.

Figure 1 can be used not only to compare the capabilities of the various modulation options but also to explore the trade-offs required to achieve a specified link gain, since each IME contour corresponds to a single value of link gain. In Fig. 1, links with high gain would fall on contours of high IME. For a given value of R, the IME is maximized by maximizing H. However, H may be fundamentally or practically limited. Therefore, to obtain the highest IME for a given H, one wants an R value as different as possible from R_{in}. Other factors, such as bandwidth, must also be considered in the choice of H and R.

III. NEW RESULTS ON EXPERIMENTAL LINKS

The experimental links reported in this section were assembled to demonstrate the enhanced performance achievable using improved devices and low-loss impedance matching. Figure 2(a) is an overview schematic of an experimental directly modulated link. A 50:12.5-Ω transformer is used for impedance matching at the laser, and the return loss is > 8 dB over the 1000-MHz bandwidth of the transformer. The photodiode has a fiber-coupled responsivity of 0.92 A/W, and its output can be measured either directly or via a 200:50-Ω transformer. The insertion gain vs frequency with the transformer input coupling to the laser is plotted in Fig. 2(b). Without the transformer output coupling from the photodiode, the insertion gain was -4.9 dB at a bandwidth of 1500 MHz; with the output transformer the gain was 0.3 dB at a bandwidth of 200 MHz. Based on the theoretical model [1], we had predicted a midband insertion gain of -4.3 dB at the wide bandwidth and a gain of 0.7 dB at the narrow bandwidth. The IME for the diode laser in this link is shown as point 3 in Fig. 1.

The link noise figures are 35.1 and 30.1 dB for the wide and narrow bandwidth cases, respectively. At these high noise levels, the major noise sources are the photodetector shot noise, the laser relative intensity noise (RIN), and the thermal noise of the photodetector load resistor. As shown in Fig. 3(a), these sources can be modeled as current sources. In Fig. 3(b), the mean-square noise currents and their sum are plotted vs average optical power on the detector, P_D, assuming a transformer turns ratio $N_D = 1$ and $R_{out} = 50\ \Omega$. For this experiment, the measured $P_D \cong 1$ mW and the RIN = -131 dB/Hz. From Fig. 3(b), we see that under these conditions the dominant noise source is the laser RIN. Recently, diode lasers with a RIN of -158 dB/Hz have been reported [5]. Such devices would produce nearly shot noise limited performance with a resulting link noise figure of 5 dB.

It is instructive to compare this performance with that of a previously reported [6] externally modulated link with a bandwidth of 150 MHz and an insertion gain of 1.0 dB. The estimated insertion gain for this link operating with a transformer-matched photodetector is 6.0 dB, and the calculated noise figure is only 15.1 dB. This noise figure is much better than that for the directly modulated link because the RIN of the solid state laser source is less than -165 dB/Hz. Thus, at a narrow bandwidth, the externally modulated link has a higher insertion gain and lower noise figure, although the same or better values appear attainable with a low-R_L, low-RIN directly modulated link.

To obtain figures for an externally modulated link operating at a wider bandwidth, we set up an experimental configuration that is the same as reported earlier [6], with two exceptions. The modulator electrodes are 13.25 mm, instead of 55 mm, and they are operated with a 50-Ω parallel match instead of a series match for wider-bandwidth operation. Also, we are using a higher-power diode-laser-pumped Nd:YAG laser capable of coupling over 100 mW, instead of 55 mW, into a single-mode, polarization-maintaining fiber. Measurements on this link are in progress, and results will be presented at the conference. Based on the link models, we anticipate an insertion gain of -1.0 dB, a 3-dB bandwidth of 800 MHz and a noise figure of 19 dB, with about 19 mW of optical power at the photodetector and a laser RIN of less than -165 dB/Hz. The performance should be nearly shot noise limited [see Fig. 3(b)]. Additional reduction in the noise figure could be achieved by increasing the modulator response, or by further increasing the laser power, since shot noise varies proportionally with P_D, but gain varies proportionally with P_D^2.

IV. SUMMARY

We have theoretically compared the factors affecting the IME for directly and externally modulated links. While the maximum electrical-to-optical conversion efficiency H with direct modulation is fundamentally limited, H for the external modulator case is limited by practical constraints, such as the maximum optical power in the MZ waveguides. However, presently these limits are higher than the fundamental limits on H for the directly modulated link. The effective input resistance R of the devices used for both modulation methods is limited by practical constraints. Consequently, the maximum matching turns ratio is also constrained. We also investigated experimentally the performance of directly and externally modulated fiber-optic links at two bandwidths. The results of these experiments are summarized in Table 1. At both bandwidths, the externally modulated link demonstrates a higher insertion gain and lower noise figure than the directly modulated link. The lower noise figure of the externally modulated link is due to the low RIN of the solid state laser used in this configuration. We expect that with a sufficient decrease in diode laser RIN, the directly modulated link will have a noise figure at least as low as that of the externally modulated link.

ACKNOWLEDGMENT

This work was sponsored by the Department of the Air Force.

REFERENCES

1. C. H. Cox III, G. E. Betts, and L. M. Johnson, "An analytic and experimental comparison of direct and external modulation in analog fiber-optic links," to appear in a special joint issue of *IEEE MTT/J. Lightwave Technol.*, vol. 38, no. 5, 1990.
2. G. P. Agrawal and N. K. Dutta, *Long-Wavelength Semiconductor Lasers*, New York: Van Nostrand Reinhold, 1986.
3. D. Z. Tsang, unpublished.
4. G. E. Betts, L. M. Johnson, C. H. Cox III, and S. D. Lowney, "High-performance optical analog link using external modulator," *Photon. Tech. Lett.*, vol. 1, pp. 404-406, 1989.
5. I. Joindot and C. Boisrobert, "Laser RIN calibration by extra noise injection," *Electron. Lett.*, vol. 25, pp. 1052-1053, 1989.
6. C. H. Cox III, L. M. Johnson, and G. E. Betts, "A theoretical and experimental comparison of directly and externally modulated fiber optic links," *IEEE MTT-S Int. Microwave Symp. Dig. II*, paper U2, 1989.